Journal of the Ceramic Society of Japan **109** [3] S43–S48 (2001)

Recent Progress in Crystal Chemistry of Belite: Intracrystalline Microtextures Induced by Phase Transformations and Application of Remelting Reaction to Improvement of Hydration Reactivity

Koichiro FUKUDA

Department of Materials Science and Engineering, Nagoya Institute of Technology, Gokiso-cho, Showa-ku, Nagoya-shi 466–8555, Japan

ビーライトの結晶化学における最近の進歩：相転移により結晶内部に形成される微細組織と再融反応を利用した水和反応性の改善

福田功一郎

名古屋工業大学材料工学科，466–8555 名古屋市昭和区御器所町

The microtextures of belite induced by a remelting reaction and other transformations (e.g., the polymorphic phase transitions of $\alpha \rightarrow \alpha' \rightarrow \beta$) have been reviewed. The remelting reaction, in which the α-phase belite decomposes into a liquid and the α'-phase during cooling, is necessarily preceded by the phase transition of $\alpha \rightarrow \alpha'$; the α'-phase nucleates as lamellae within the parent α-phase so that there is good lattice matching across the interface. The resulting lamella boundaries provide heterogeneous nucleation sites for the exsolving liquid by the remelting reaction. A variety of microtextures results depending on the wettability of the belite lamellae by the exsolved liquid as well as on the cooling rate. The belite in which the remelting reaction occurred to a large extent showed higher hydration reactivity and better grindability than the quenched material. Recent years have seen developments in a new application for the remelting reaction that involves modifying belite-rich cement.

[Received October 2, 2000]

Key-words : *Belite, Crystal chemistry, Remelting reaction, Phase transformations, Microtextures, Hydration*

1. Introduction

THE *remelting reaction* is an unusual decomposition reaction, in which a solid decomposes into a liquid and another solid during cooling. The reaction rarely occurs in alloys, for example, of the binary systems Fe–S, Cu–Sn and Mn–Zn. With the silicates other than belite (Ca_2SiO_4 solid solution), the reaction has never been reported.[1)–5)] Belite is a main constituent of normal Portland cement clinkers, of which it constitutes 15–30 mass%. The crystal chemistry has been extensively studied for over a century since the cements were designed for general constructional use.[6)–10)] However, the remelting reaction of belite was never recognized until 1992,[1)] despite its great importance in the crystal chemistry as well as in the hydration kinetics.

Attention has been given to cements in which the major constituent is belite.[11)] This is partly because the belite-rich cement, the belite content of which ranges from ~50 to ~80 mass%, promises better environmental protection, including the reduction of CO_2 gas emission and the conservation of raw materials. However, the main problems in the practical use of belite-rich cement are a low hydration reactivity and a strong resistance to fracture on grinding. Recently, the belite in which the remelting reaction sufficiently occurred (remelted belite) has been revealed to show higher hydration reactivity and better grindability than the quenched material.[12)–14)] Both properties are closely related to the belite microtextures induced by the remelting reaction.

Highly reactive β-Ca_2SiO_4 crystals without any foreign oxides have been, on a laboratory scale, successfully synthesized by a sol–gel-type method and hydrothermal processing.[15)–18)] The reactivity in such cases is effectively increased by the high specific surface area of the powder specimens. On the other hand, the cement rich in the remelted belite (remelted belite cement) was prepared from the starting materials of the industrial belite-rich cement clinkers.[13)] This implies that the mass production of the modified cement on an industrial scale could be practical. The remelted belite cement could therefore be a new type of high-performance cement in the future rather than an advanced substitute for the conventional belite-rich cement.

The polymorphic sequence and crystal structures of belite have been considered to be analogous to those of pure Ca_2SiO_4, of which the polymorphs (Fig. 1) established so far are, at ordinary pressures, γ (orthorhombic), α'_L (orthorhombic), α'_H (orthorhombic) and α (trigonal) in the order of increasing temperature.[11)] The β-phase (monoclinic), stable at high pressures, occurs on rapid cooling. In normally processed Portland cement clinkers, the belite contains enough foreign oxides and is free of the transformation to the γ-phase, which is unreactive with water. The γ-phase is much less dense than the β-phase so that this transformation causes the crystals of the β-phase to disintegrate into fine powders, a phenomenon known as dusting. A one-dimensional modulated structure has been observed in a polymorph of belite, which contains certain foreign oxides (e.g., P_2O_5) in limited concentration ranges.[19)]

In the present paper, the author has reviewed the transformation-induced microtextures of belite, followed by a new application for the remelting reaction that involves modifying the reactivity of the belite-rich cement. The

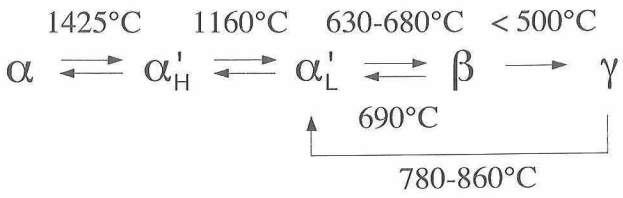

Fig. 1. Polymorphism of Ca_2SiO_4.[11)]

remelting reaction necessarily is preceded by the polymorphic phase transition of $\alpha \rightarrow \alpha'_H$. The subsequent transformation of $\alpha'_L \rightarrow \beta$ has been reported to be thermoelastic as well as martensitic. The remelting reaction requires atomic diffusion, while the rest involves no diffusion process. Because the α'_H-to-α'_L transition does not affect the relevant microtextures, both phases are simply represented by α'.

2. Nucleation of new phases and their morphology

In nucleation and growth transformations, the overall free energy change (ΔG_{Total}) with the formation of the new phase within the host crystal comprises the volume (ΔG_{Volume}), surface ($\Delta G_{Surface}$) and strain energy (ΔG_{Strain}) terms:[20]

$$\Delta G_{Total} = \Delta G_{Volume} + \Delta G_{Surface} + \Delta G_{Strain}.$$

The morphology of the new phase should be determined so as to make the last two terms minimal. When the strain energy is important, the new phase may be oriented in the form of lamellae within the matrix so that there is good lattice matching across the interface. If the surface energy is important and also isotropic, the precipitated phase can be spherical in shape as liquid droplets. Situations similar in principle to those described above are the α-to-α' polymorphic phase transition for the former and the remelting reaction for the latter.

3. α-to-α' polymorphic phase transition

3.1 Orientation of α'-phase lamellae in host α-phase

The α-to-α' polymorphic phase transition is accompanied by the formation of the intracrystalline lamella structure; the α'-phase nucleates as lamellae in the host α-phase. The overall lamella structure was determined by the stereographic analysis of the observed lamella orientation.[21] The results showed that there are six sets of crystallographically equivalent lamellae, each of which is parallel to $\langle 210 \rangle_\alpha$ and intersects $(001)_\alpha$ at an angle of $27 \pm 3°$ (Fig. 2). During further cooling, the α'-phase often is inverted to the β-phase, leading to the formation of polysynthetic twinning at the submicroscopic level within each lamella.

Perfectly coherent interphase boundaries are expected between the α'-phase lamellae and the α-phase host. The orientation of such coherent interfaces was found from calculation based on the matrix algebra analysis as used in martensitic transformations.[22),23)] The calculation procedure requires only the lattice parameters of both phases and their lattice correspondence,[24)-26)] which is expressed by $\{1120\}_\alpha // (100)_{\alpha'}$ and $[0001]_\alpha // [001]_{\alpha'}$.

Because of the trigonal symmetry for the parent α-phase, there are six symmetrically related sets of interfaces in all, which intersect $(001)_\alpha$ at 26.8° (Fig. 3).[22] This is in fair agreement with 27° obtained experimentally. In a similar manner, the intersection angle of $29.3 \pm 0.3°$ is obtained as the most probable one at the transition temperature,[23] taking into consideration the temperature dependence of cell parameters for the α- and α'-phases.[27]

3.2 Kinetics

The α-to-α' transition in belite is a nucleation and growth process. Thus the transition process can be shown on a time–temperature–transformation (TTT) diagram.[28] The two C-shaped curves in Fig. 4(a), respectively, give the relation between time and temperature for the start (left) and the finish (right) of the transition. In the region between the two curves, the belite is composed of both the α- and α'-phases, and the fraction of α' increases with time for a given temperature. The broken line in the figure gives the thermodynamic transition temperature between α and α' (T_c); the α'-phase exists in equilibrium with the parent α-phase at ~1280°C. The temperature at which the transition occurs at a maximum rate lies at ~1100°C. Below the kinetic cut-off temperature of ~700°C, the transition becomes virtually unobserved.

In general, the rate of transformation in a nucleation and growth process depends on the rate of stable nuclei formation and their subsequent growth rate.[20] Taking only the thermodynamic factor into account, the rate equation for the overall transformation is expressed as

$$I = K \cdot \exp(-\Delta G(T)/RT) \exp(-H/RT)$$

where ΔG and H are, respectively, the activation energies for nucleation and growth of the α'-phase, R the gas constant and K a constant. The pre-exponential term K includes the thermal entropy term (S), and hence H is used instead of G ($=H-TS$). The ΔG and H values can be determined on the assumption that the time t for a given fraction of transition is inversely proportional to the nucleation rate. Putnis and McConnell[20] give the solution as:

$$H = R[\mathrm{d}(\ln t)/\mathrm{d}(1/T)] \text{ for low } T \quad (1)$$

$$\Delta G(T) = RT(\Delta \ln t) \quad (2)$$

Equation (1) shows that, when the starting curve in Fig. 4(a) is re-plotted against $\ln t$ and $1/T$, the H value can be obtained from the slope of the linear part of the curve at low temperatures (Fig. 4(b)). Equation (2) shows that, for a given temperature, the ΔG value is derived from the distance ($\Delta \ln t$) between the extrapolated straight line and the

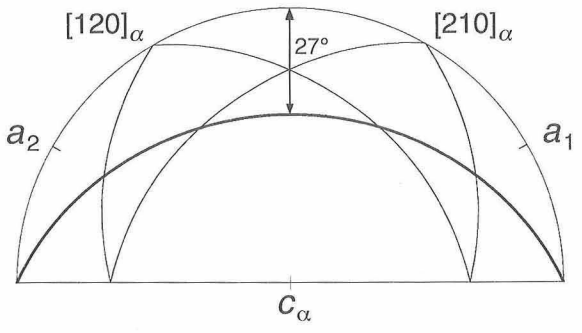

Fig. 2. Stereographic drawing of six symmetrically related α'-phase lamellae in the host α-phase. The lamellae are parallel to $\langle 210 \rangle_\alpha$ and intersect at 27° with $(001)_\alpha$. The great circle drawn in a solid line represents one of the six lamellae.

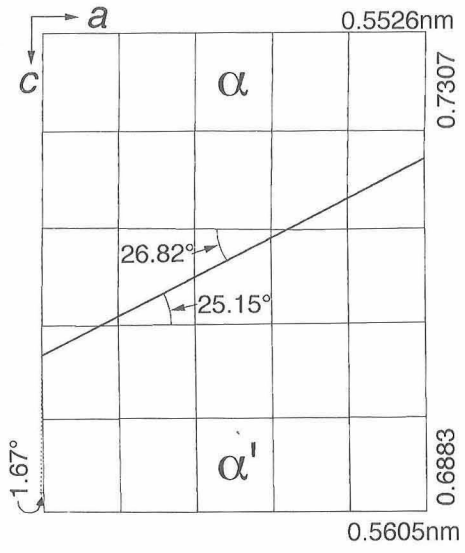

Fig. 3. Lattices of the α- and α'-phases fitted together at the coherent interface. The interphase boundary forms an angle of 26.8° with $(001)_\alpha$.

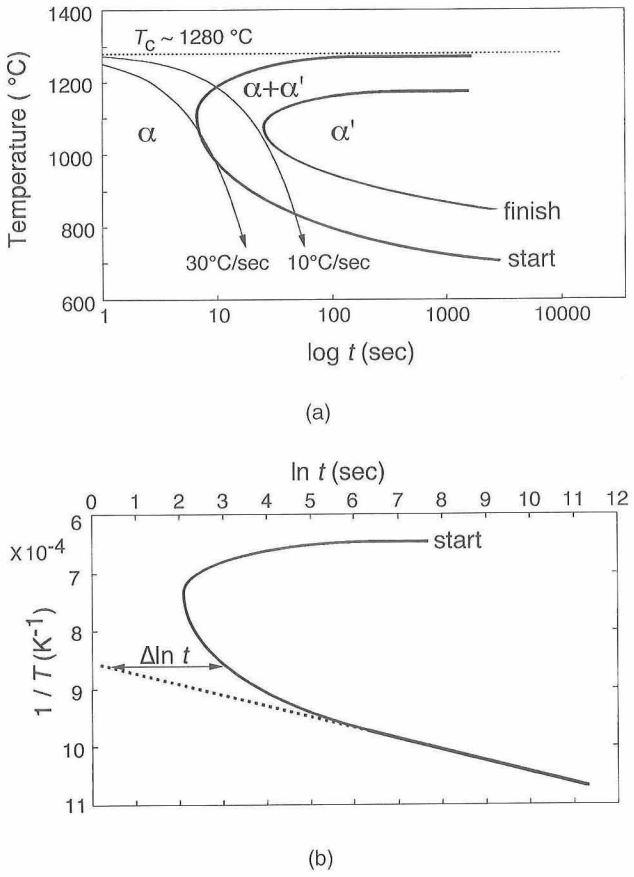

Fig. 4. (a) Time-temperature-transformation diagram for the α-to-α' polymorphic phase transition. The cooling curves are for the linear cooling from T_c (~1280°C). (b) Starting curve replotted against ln time and $1/T$ (K^{-1}). The H value is found to be 350 KJ·mol^{-1}. Sample with chemical formula of $(Ca_{1.87}Na_{0.13})_{\Sigma 2}(Si_{0.90}Al_{0.04}Fe_{0.03})_{\Sigma 0.97}O_{3.83}$.

curve as in Fig. 4(b).

By superposing cooling curves on the TTT diagram, we can predict the intracrystalline microtexture as well as the constituent phases. The cooling curves in Fig. 4(a) are for the linear rates of 30°C/s and 10°C/s from T_c. The curve for a rate higher than 30°C/s does not cross the starting curve, and hence only the α-phase is obtained at ambient temperature. For a cooling rate between 30°C/s and 10°C/s, the transition starts at ~1150°C, though the transition is not completed. Accordingly, the crystal grains will show the lamella structure consisting of both the α- and α'-phases. For a cooling rate lower than 10°C/s, the α-phase will be entirely inverted to the α'-phase. After the completion of the transition, the remelting reaction, as mentioned below, will immediately occur within the crystal.

4. Remelting reaction

4.1 Phase stability

The CaO–SiO_2–Al_2O_3 ternary phase diagram[29] shows that the liquidus field of Ca_2SiO_4 extends toward the $Ca_{12}Al_{14}O_{33}$ component; the liquid coexisting with Ca_2SiO_4 varies in composition along the line Ca_2SiO_4–$Ca_{12}Al_{14}O_{33}$. Thus, the phase stability study has been done in this pseudo-binary system to confirm the remelting reaction of the α-phase belite (Fig. 5(a)).[30]

To illustrate an ideal sequence of the cooling process in the system, we will consider the changes which take place in the α-phase crystal coexisting with a liquid at a temperature A in Fig. 5(b). When the crystal, of which the $Ca_{12}Al_{14}O_{33}$ content is 2.5 mass%, is cooled rapidly between the temperatures C (1395°C) and D (1348°C), it decomposes into a liquid and the α'-phase, the $Ca_{12}Al_{14}O_{33}$ content of which (~1 mass%) is lower than the parent α-phase. This reaction is termed remelting. The remelting reaction ceases at 1348°C, and the end result is the mixture of the α'-phase and the liquid. The proportion of each, as determined by the lever rule, is ~98 mass% of the α'-phase and ~2 mass% of the liquid. The liquid consists of ~17.5 mass% Ca_2SiO_4 and ~82.5 mass% $Ca_{12}Al_{14}O_{33}$.

4.2 Alternative metastable behavior during cooling

The direct transformation of $\alpha \rightarrow$ liquid + α' shown in the diagram, however, seems to require a large activation energy. Accordingly, the α-to-α' polymorphic transition first occurs upon cooling without a change in chemical composition.[31] Note that the resulting α'-phase is not a stable phase and represents a kinetically more favorable method of reducing the overall free energy, having failed in the thermodynamically more advantageous transformation to liquid + α'. This type of behavior is termed *alternative metastable behavior*.[20] After the transition, the liquid exsolves heterogeneously on the lamella boundaries because of the favorable activation energy for nucleation.[1]

The α-phase crystal, as it cooled from the temperature A, will ideally decompose into the α- and α'-phases between the temperatures B and C (Fig. 5(b)). However, unless the cooling rate is extremely slow, this reaction will not virtually occur. This is because the decomposition reaction requires an atomic diffusion process in solids and therefore is sluggish.

4.3 Wettability of belite lamellae by exsolved liquid

The rate of the remelting reaction depends not only on the temperature but also on the wettability of the α'-phase lamellae by the exsolved liquid.[2),3] The difference in wettability should come from the chemical composition of the exsolved liquid, which is determined by the types of impurities and their relative concentration (Al/Fe ratio) in the parent α-phase belite.

The belite with Al/Fe (molar ratio) <1 exsolves the liquid with low wettability. Thus the liquid forms droplets on the lamella boundaries (Fig. 6(a)).[1] These droplets with minimum interfacial area would readily reach a local equilibrium with the surrounding belite matrix. Inside the lamellae, the remelting reaction would not occur because of the large activation energy for homogeneous nucleation of the liquid. Under these conditions, the rate-determining step is the volume diffusion of foreign ions from the bulk to the liquid droplets on the lamella surfaces, and thus the reaction is very sluggish. The reaction rate after the formation of the droplets is so low that the outline of the original belite grains and the intracrystalline lamella structure tend to remain despite slow cooling.

The liquid, which is exsolved from the belite with Al/Fe >1, has high wettability. Hence, it readily spreads over the lamellae and disintegrates the lamella structure.[2] Because the large interfacial area is invariably kept between the lamellae and the liquid, the reaction proceeds until the parent crystals are completely replaced by the new α'-phase belite (Fig. 6(b)). During the decomposition process, the impurity concentration continues to decrease and various microtextures, as described in the literatures,[32)-35] result.

When the liquid coexisting with the α-phase crystal at the temperature A in Fig. 5(b) is cooled, the α'-phase crystal will be newly nucleated from the liquid between the temperatures C and D. The crystals that are precipitated in this manner are usually observed as overgrowths on the former α-phase crystals (Fig. 6(b)).[2] During further cooling, the transition of $\alpha' \rightarrow \beta$ occurs both in the remelted and over-

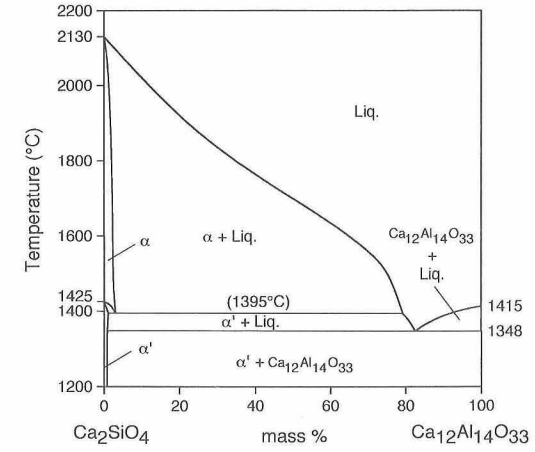

(a)

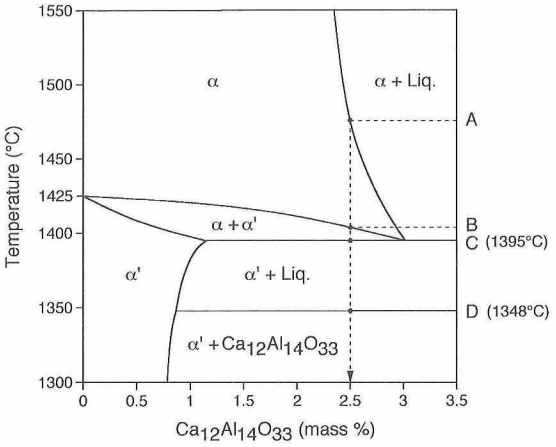

(b)

Fig. 5. (a) Phase diagram of P_2O_5-bearing pseudobinary Ca_2SiO_4–$Ca_{12}Al_{14}O_{33}$ system showing the occurrence of the remelting reaction in the α-Ca_2SiO_4 solid solution. No phase distinction is made between α'_H and α'_L, and both are simply represented by α'. A small amount of P_2O_5 is added to prevent the pulverization of the belite crystals due to the β-to-γ phase transition upon quenching. (b) Part of the Ca_2SiO_4–$Ca_{12}Al_{14}O_{33}$ system in (a), showing that the single α-phase decomposes into the two-phase mixture of α' and liquid upon cooling between the temperatures C and D.

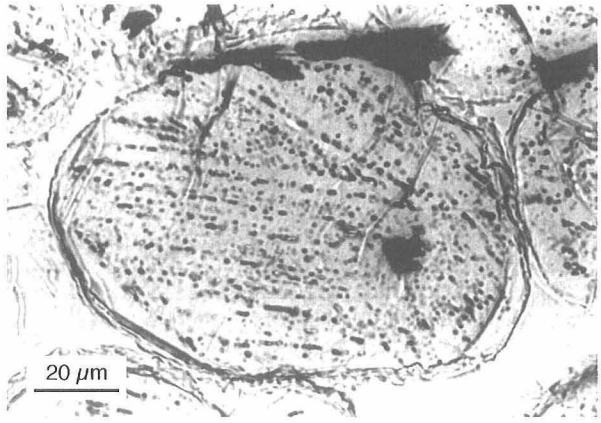

(a)

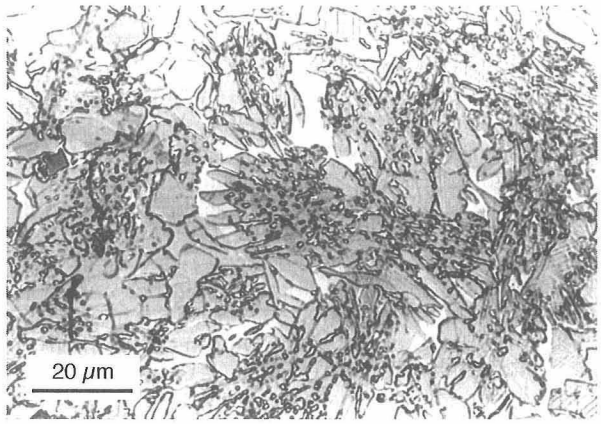

(b)

Fig. 6. Optical micrographs showing belite microtextures induced by the remelting reaction. (a) Belite crystals with Al/Fe (parent α-phase) <1. Transmitted light. The liquid droplets are disposed in lines on the lamella boundaries, indicating that they heterogeneously nucleate on the boundaries after the α-to-α' polymorphic transition. (b) Belite crystals with Al/Fe (parent α-phase) >1 in an industrial Portland cement clinker. Reflected light. Etched with nital. The parent α-phase crystals are completely melted and replaced by the new α'-phase (now β-phase) crystals.

grown crystals, leading to the formation of the polysynthetic twinning frequently on $(100)_\beta$ and rarely on $(001)_\beta$.[36]

4.4 Kinetics

The quantitative relationship between the fraction remelted and the cooling rate was determined for the belite doped with Na_2O, Al_2O_3 and Fe_2O_3.[5] Because the Al/Fe molar ratio of the parent belite was larger than unity, the impurity concentration continued to decrease during the decomposition process. The β-angle varied most sensitively with the Na/(Na+Ca) ratio ($=x$) according to

$$\beta(^\circ) = 94.55 - 8.86x \quad (0 \leq x \leq 0.03).$$

The decrease in x caused by the remelting reaction was therefore detectable by the increase in β. When the belite was cooled at a constant rate r(°C/s) over the temperature range in which the remelting reaction occurred, the fraction remelted (ζ) was expressed by

$$\zeta = 1 - \exp(-1.33\, r^{-0.25}).$$

It is noted that this rate equation must be modified on application to the belite with different types of foreign oxides.

5. Application of remelting reaction to improvement of hydration reactivity and grindability

5.1 Hydration behavior of remelted belite

Recently, the hydration reactivity and grindability of the belite-rich cement have been effectively improved by the remelting reaction of the constituent belite.[12)-14)] The modified cement, termed remelted belite cement, is mainly composed of belite in which the remelting reaction occurred to a large extent and is thus distinct from the conventional belite-rich cement. The remelted belite consisted of the polysynthetically twinned β-phase, together with the exsolved liquid in high alkali concentration. On the other hand, the conventional belite-rich cement, of which the constituent belite was rapidly quenched to depress the occurrence of the remelting reaction, contained the alkalies (and the other foreign oxides) in solid solution to occasionally stabilize the α'-phase.

The rate of heat evolution at 20°C has been, for example, compared between the modified and conventional belite-rich cements (Fig. 7).[14] The main heat evolution peak of the former began ~7 h earlier and rose more steeply than that of the latter. Because the two cements showed nearly the

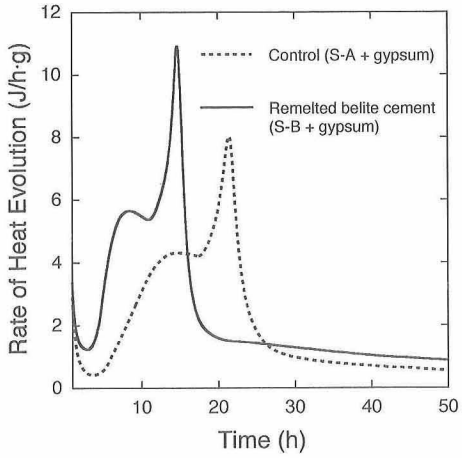

Fig. 7. Rate of heat evolution at 20℃ and water/cement = 0.5 by weight.[14] Sample S–A is analogous to the conventional belite-rich cement cliker, and that of S–B is mainly composed of the remelted belite crystals.

same specific surface areas as well as very similar particle size fractions, the difference in hydration behavior between them is independent of their powder properties. Accordingly, the early hydration reactivity, evaluated from the heat evolution, was higher for the former than for the latter.

5.2 Hydration accelerators

In general, the rate of cement hydration is significantly increased by the dissolved alkalies in the water in contact with hydrating cement.[37] When the remelted belite crystals, together with the exsolved liquid (a solid at ambient temperature), are finely pulverized and mixed with water, the exsolved alkalies would readily dissolve into the water. This leads to the high reactivity during the initial stage of the cement hydration.[13),14]

The grindability of belite-rich cement has been markedly increased by the remelting reaction.[12)-14] The better grindability was derived from the weaker resistance to fracture for the remelted belite compared to the quenched material. The resulting powder specimen of the former showed higher specific surface area than that of the latter, which effectively improved the early hydration reactivity.

The hydration behavior has been compared between the α'- and twinned β-phases with identical chemical compositions.[38] With pulverized crystals, the intersections of the twin boundaries and the crystal surface behaved like active centers of the reaction with water. The β-phase, therefore, showed a much higher hydration reactivity than the α'-phase during the early stage of the hydration process. In a manner similar to that above, the hydration reactivity of the remelted belite consisting of the twinned β-phase was much higher than that of the quenched material mainly consisting of the α'-phase.[14]

The probable hydration accelerators of the remelted belite proposed so far are the exsolved liquid rich in alkalies, the high specific surface area of the pulverized crystals, and the twin boundaries of the β-phase. However, the detailed hydration mechanism of the remelted belite needs to be investigated further. The complete clarification could enable the modified belite-rich cement to be practical on an industrial scale.

6. Miscellaneous transformations

6.1 Thermoelastic martensitic transformation

In a martensitic reaction, the cooperative movement of many thousands of atoms occurs.[39] Thus, the relief effect on the parent crystal surface is characteristic of such a transformation.

The α'-to-β transformation has been reported to be martensitic.[40)-43] The surface relief induced by the transformation was quantitatively investigated on a nanometer scale using an atomic force microscope.[44] The surface relief angle was determined from the observation to compare with that found from calculation based on the phenomenological theory.[45),46] The fair agreement between them implied that the transformation is definitely martensitic and mainly governed by a shear mechanism. With ceramic materials other than belite, the martensitic behavior, which is non-thermoelastic, is well-known to occur in zirconia.

In situ observation has been made, under a high-temperature optical microscope, of the prepolished surface of the parent α'-phase belite.[47] The transformation proceeded with the growth of the martensite (β-phase) plates during cooling. The growth ceased when cooling was stopped and resumed upon further cooling. Upon heating, the plate formed last during cooling began to disappear, and the original flat surface was eventually restored. The behavior of this kind is termed *shape memory effect*. Upon repeated heating and cooling cycles, the transformation was completely reversible.

The transformation temperatures have been determined to show the thermal hysteresis (A_s–M_s) as being negative, where A_s and M_s are respectively the starting temperatures of the reverse (β-to-α') and forward (α'-to-β) transformations.[48] The negative thermal hysteresis as well as the growth and shrinkage behavior of the martensite plates strongly suggest that the transformation is thermoelastic.[45)-49]

6.2 Incommensurate phase transformation

An orthorhombic incommensurate superstructure has been observed in the belites doped with P_2O_5 and/or other oxides.[19),50)-55] This phase appears when the parent α-phase fails to undergo the α-to-α' transition on quenching. The crystal grain consists of domains related by 120° rotation around the c-axis of the former α-phase.[19] The domains were at the submicroscopic level with irregular domain boundaries. Thus, the crystal grains showed mottled extinction under crossed polars. The electron diffraction pattern has revealed that the modulation is one-dimensional and that all the reflections are expressed by

$$Q = h\mathrm{a}^* + k\mathrm{b}^* + l\mathrm{c}^* + n\mathrm{k}$$

using four indices (h, k, l, and n), where k is the wave vector.[54] This vector is redefined using the modulation wavelength N and the unit vectors a* and c* as $(1/N)\mathrm{a}^* + \mathrm{c}^*$. A good correlation between N and P/(Si+P) indicates that a commensurate phase with $N=4$ exists at P/(Si+P) = 0.148. The crystal structure may be close to that of $6Ca_2SiO_4 \cdot Ca_3(PO_4)_2$ (P/(Si+P) = 0.250 and $N=3.75$), of which structural refinement was made assuming $N=4$.[51]

6.3 Transformations of belite in normal cement clinkers

The belite in industrial Portland cement clinkers is mostly formed in the stable temperature region of the α-phase. When the belite, containing a large amount of impurities, is cooled rapidly, the α-to-α' phase transition can be incomplete. The resulting belite is therefore composed of the α'-phase lamellae and the host α-phase. Upon subsequent cooling, the α'-phase is inverted to the β-phase. The end result at ambient temperature is the belite composed of both the α- and β-phases. With slower cooling, the initial α-phase belite can be completely inverted to the α'-phase. Immediately after completion of the transition, the remelting reaction occurs heterogeneously on the lamella boundaries. The resulting microtexture mainly depends on the Al/Fe ratio of the parent α-phase as well as on the cooling rate.

Acknowledgment The author thanks Emeritus Professor Iwao Maki and Dr. Suketoshi Ito, Nagoya Institute of Technology, for productive discussions.

References

1) Fukuda, K., Maki, I. and Ito, S., *J. Am. Ceram. Soc.*, 75, 2896–98 (1992).
2) Fukuda, K., Maki, I., Ikeda, S. and Ito, S., *J. Am. Ceram. Soc.*, 76, 2942–44 (1993).
3) Fukuda, K., Maki, I., Ito, S., Yoshida, H. and Kato, C., *J. Am. Ceram. Soc.*, 77, 3027–29 (1994).
4) Fukuda, K., Maki, I., Ito, S. and Yoshida, H., *J. Am. Ceram. Soc.*, 78, 3387–89 (1995).
5) Fukuda, K., Maki, I., Ito, S. and Toyoda, K., *J. Ceram. Soc. Japan*, 103, 444–48 (1995).
6) Bredig, M. A., *J. Am. Ceram. Soc.*, 33, 188–92 (1950).
7) Yamaguchi, G., Ono, Y., Kawamura, S. and Soda, Y., *J. Ceram. Assoc. Japan* (*Yogyo-Kyokai-Shi*), 71, 105–08 (1963) [in Japanese].
8) Niesel, K. and Thorman, P., *Tonind. Zeitung*, 91, 362–69 (1967).
9) Regourd, M., Bigare, M., Forest, J. and Guinier, A., Proc. 5th Int. Symp. Chem. Cement, Tokyo, Vol. 1 (1968) pp. 44–48.
10) Ghosh, S. N., Rao, P. B., Paul, A. K. and Raina, K., *J. Mater. Sci.*, 14, 1554–66 (1979).
11) Taylor, H. F. W., "Cement Chemistry," 2nd ed., Thomas Telford, London, U. K. (1997).
12) Fukuda, K. and Ito, S., *J. Am. Ceram. Soc.*, 82, 637–40 (1999).
13) Fukuda, K. and Ito, S., *J. Am. Ceram. Soc.*, 82, 2177–80 (1999).
14) Fukuda, K., Wakamatsu, N., Ito, S. and Yoshida, H., *J. Ceram. Soc. Japan*, 107, 901–06 (1999).
15) Roy, D. M. and Oyefesobi, S. O., *J. Am. Ceram. Soc.*, 60, 178–80 (1977).
16) Ishida, H., Sasaki, K. and Mitsuda, T., *J. Am. Ceram. Soc.*, 75, 353–58 (1992).
17) Ishida, H., Mabuchi, K., Sasaki, K. and Mitsuda, T., *J. Am. Ceram. Soc.*, 75, 2427–32 (1992).
18) Okada, Y., Ishida, H., Sasaki, K., Young, J. F. and Mitsuda, T., *J. Am. Ceram. Soc.*, 77, 1313–18 (1994).
19) Fukuda, K. and Maki, I., *J. Am. Ceram. Soc.*, 72, 2204–07 (1989).
20) Putnis, A. and McConnell, J. D. C., "Principles of Mineral Behaviour," Backwell Scientific Publications, Oxford, U. K. (1980).
21) Fukuda, K. and Maki, I., *Cem. Concr. Res.*, 19, 913–18 (1989).
22) Fukuda, K. and Maki, I., *Cem. Concr. Res.*, 23, 599–602 (1993).
23) Fukuda, K., *Cem. Concr. Res.*, 28, 1105–08 (1998).
24) Bowles, J. S. and Mackenzie, J. K., *Acta Metal.*, 2, 129–37 (1954).
25) Mackenzie, J. K. and Bowles, J. S., *Acta Metal.*, 2, 138–47 (1954).
26) Wayman, C. M., "Introduction to the Crystallography of Martensitic Transformations," The Macmillan Company, New York (1964).
27) Remy, C., Andrault, D. and Madon, M., *J. Am. Ceram. Soc.*, 80, 851–60 (1997).
28) Fukuda, K., Maki, I., Toyoda, K. and Ito, S., *J. Am. Ceram. Soc.*, 76, 1821–24 (1993).
29) Osborn, E. F. and Muan, A., "Phase Diagrams for Ceramists," Ed. Reser, M. K., Am. Ceram. Soc., Columbus, OH (1964) Fig. 630.
30) Fukuda, K., Takeda, A. and Yoshida, H., in preparation.
31) Fukuda, K., Maki, I. and Ito, S., "Transformation-Induced Microtextures in Belite"; pp. li52 in Proceedings of 10th International Congress on the Chemistry of Cement (Sweden, 1997). Amarkai AB and Congrex Goteborg AB, Goteborg, Sweden (1997).
32) Insley, H., *J. Res. Natl. Bur. Stand.*, 17, 353–61 (1936).
33) Insley, H., Flint, E. P., Newman, E. S. and Swenson, J. A., *J. Res. Natl. Bur. Stand.*, 21, 355–65 (1938).
34) Barnes, P. and Ghose, A., (Barnes, P. (Ed)): "The Microscopy of Unhydrated Portland Cement," Structure and Performance of Cements. Applied Science Publishers, U.K. (1983) pp. 139–203.
35) Fukuda, K., *J. Mineral. Soc. Japan*, 23, 179–88 (1994) (in Japanese).
36) Kim, Y. J., Nettleship, I. and Kriven, W. M., *J. Am. Ceram. Soc.*, 75, 2407–19 (1992).
37) Jawed, I. and Skalny, J., *Cem. Concr. Res.*, 8, 37–52 (1978).
38) Fukuda, K. and Taguchi, H., *Cem. Concr. Res.*, 29, 503–06 (1999).
39) Delaey, L., "Diffusionless Transformations," in Phase Transformations in Materials, VCH, Weinheim (1991) pp. 339–404. (Hassen, P. (Ed))
40) Groves, G. W., *J. Mater. Sci.*, 16, 1063–70 (1981).
41) Groves, G. W., *Cem. Concr. Res.*, 12, 619–24 (1982).
42) Groves, G. W., *J. Mater. Sci.*, 18, 1615–24 (1983).
43) Fukuda, K., Iizuka, E., Taguchi, H. and Ito, S., *J. Am. Ceram. Soc.*, 81, 2729–31 (1998).
44) Fukuda, K., Taguchi, H., Nomura, Y. and Ota, T., *J. Am. Ceram. Soc.*, 83, 2097–99 (2000).
45) Fukuda, K., *J. Mater. Res.*, 14, 460–64 (1999).
46) Fukuda, K., *J. Ceram. Soc. Japan*, 108, 701–04 (2000).
47) Fukuda, K., Maki, I. and Ito, S., *J. Am. Ceram. Soc.*, 79, 2925–28 (1996).
48) Fukuda, K., Maki, I. and Ito, S., *J. Am. Ceram. Soc.*, 79, 2969–70 (1996).
49) Fukuda, K., Ito, S. and Taguchi, H., *Cem. Concr. Res.*, 28, 1141–45 (1998).
50) Saalfeld, H., *Z. Kristallogr.*, 133, 396–404 (1971).
51) Saalfeld, H. and Klaska, K. H., *Z. Kristallogr.*, 155, 65–73 (1981).
52) Jelenic, I. and Bezjak, A., *Cem. Concr. Res.*, 12, 785–88 (1982).
53) Fukuda, K., Maki, I. and Adachi, K., *J. Am. Ceram. Soc.*, 75, 884–88 (1992).
54) Fukuda, K., Maki, I., Ito, S., Yoshida, H. and Aoki, K., *J. Am. Ceram. Soc.*, 77, 2615–19 (1994).
55) Fukuda, K., Maki, I., Ito, S. and Miyake, T., *J. Ceram. Soc. Japan*, 105, 117–21 (1997).

Associate professor Fukuda received his BS, MS, and Dr from the University of Tokyo, Japan. In 1986, he became a research associate at Nagoya Institute of Technology. From 1997 to 1998, he was a research fellow in the Department of Chemistry at the University of Aberdeen, UK. He received the Research Paper Award of the Year from the Mineralogical Society of Japan in 1989, and the CerSJ Award for Advancement in Ceramic Science and Technology from the Ceramic Society of Japan in 1996.